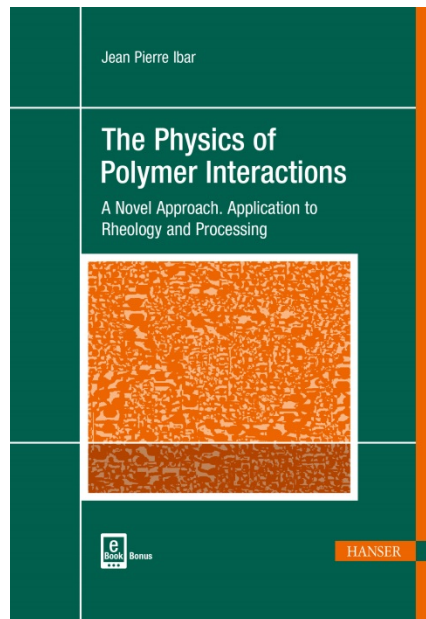


HANSER



Sample Pages

The Physics of Polymer Interactions

Jean Pierre Ibar

ISBN (Book): 978-1-56990-710-8

ISBN (E-Book): 978-1-56990-711-5

For further information and order see

www.hanserpublications.com (in the Americas)

www.hanser-fachbuch.de (outside the Americas)

© Carl Hanser Verlag, München

Preface

Forty Years of Painting on the Same Canvas

It seems that my life for the last 40 years has been dedicated to the understanding of ideas I once conceived while student at M.I.T. [1]. These initial ideas were intuitive at first but evolved into a school of thoughts which are now grounded in me as the basis for a philosophy of life.

I realize in writing this preface for this book how much the story of my life has been driven by this intensely creative time spent while I was 22-25 years old, possibly triggered by my fortuitous presence at this prestigious institution and also inspired by the air of the time, in the post-hippie generation, which I had fully discovered and endorsed. It was also during this extraordinarily focused time that I met the person who became my dear wife and the closest witness of my evolution and of its implications in our daily life.

My supervisor at M.I.T. was at first Prof. E.W. Merrill, a true gentleman and a very good teacher. But the tuition was expensive and Prof. Fred McGarry had convinced me - by giving me a teaching assistantship - that he should become my supervisor. He also opened up his contacts allowing me to meet and work with prestigious scientists such as R.F. Boyer and Turner Alfrey at the Dow Research Center (Midland, MI), and Profs. Bruce Maxwell and John Gillham at Princeton. He may also have had another agenda in mind when he introduced me to his family of six daughters, several of whom were approximately my age, students at Radcliff, beautiful and interesting young women who had just lost their mother to cancer, herself a talented French and Spanish professor at Radcliff. In any case, history cannot be re-written and, at the end, my supervisor and father of these beautiful young women from Radcliff, refused to sign my thesis dissertation, although it was listed for graduation in May 1975.¹ I can only blame myself: he who plays with fire accepts the possibility to get burned! Yet, over 40 years later, I consider that not having my M.I.T thesis validated officially at the time, whatever the true reasons, pushed me to improve it for all these years. Furthermore, to demonstrate that it

¹ The PhD degree was finally granted to me by UPV/EHU 42 years later.

had merits may have been the driving force leading to new discoveries which, in turn, resulted in improvements of the original concepts.

The research I started, just after M.I.T., on the use of vibration in molding processes, led to the “Rheomolding” and, more recently, to the “Rheo-Fluidification” technologies which are currently in use in industry to help plastics processors and compounders. The TSC/RMA spectrometer which I developed under license from Prof. C. Lacabane and commercialized in the 1990s stemmed from my interest in characterizing coupled and interactive molecular motions in terms of the new theory of polymer physics I had initiated at M.I.T.

From 1976 to 2006 I had the chance and privilege to merge an interesting and challenging career as an entrepreneur developing projects and instruments directly resulting from and testing my new theoretical ideas in polymer physics, and the continuing theoretical research which demanded the improvement and generalization of those new ideas. Since 2007 I have turned my attention entirely to polymer physics from an academic standpoint, first by catching up with the academic world and studying how it had advanced since 1975, then by trying to combine theoretically what 15 years of experiments in solid state amorphous matter had taught me with another 15 years of experiments in melt flow dynamics (rheological experiments and processing manipulation). This is where I stand right now. In a certain sense, I have the clear impression that I have spent 40 years re-thinking, modifying, and re-writing my M.I.T. thesis, like a painter who would have spent his life re-touching over and over the same painting.

1. The M.I.T Thesis: “A Theory for the Properties and the Behavior of Polymeric Materials”

My PhD dissertation at M.I.T (1975) presented the first version of what I now call “the Grain-Field-Statistics”, the basis for my proposed new theory of polymer physics and the subject of this research. The conformational statistics of “bond-units”, which were defined along a single chain without intermolecular interactions, could be represented with a multi-conformational state model, similar to the type used by Volkenstein [2] or Robertson [3, 4]. The effect of the inter-molecular interactions between the bond-units, belonging or not to the same macromolecule, was perceived as the influence on each other of randomly distributed bond-units assuming all types of conformations without any preference, creating nodules of bond-units called “bb-balls” (bonded-bonds). The bb-balls gathered into systems, “Energetic Kinetic Systems”, which were thermodynamically stable because of the formation of a few bonds of a special type, of lower conformation energy, i.e. of bond-units assuming the same and most stable conformation, trans or helicoidal for instance. This speculative interpretation of the Energetic Kinetic Network Theory resulted in the creation of “local order” in the morphology, which was presented as plate-like bundles, small enough to be invisible to the microscopists ($< 60 \text{ \AA}$), and of nodules

of randomly packed bonds surrounded at their interface by “free bonds”. The size and shape of the bb nodules depended on the temperature and the amount of orientation. The macromolecules were wandering around, participating partially in the buildup of the bb balls, and more scarcely to the bundles, at least in the case of true amorphous polymers (Figure 1).

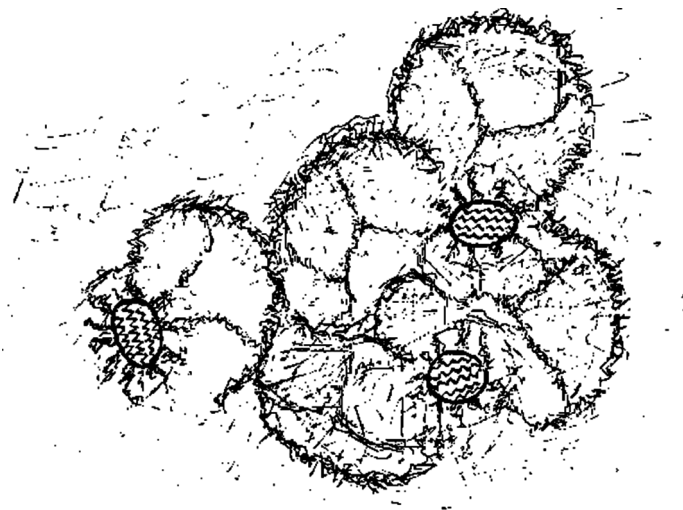


Figure 1 Sketch representing the morphology of amorphous polymers, from 1975 thesis

The Energetic Kinetic Systems were defined by the ensemble of bond-units in a group of nodules and their interface, stabilized by the presence of two adjacent bundles, so the stability of the systems was really the result of the existence of the bundles themselves. $T_{L,L}$ was the temperature of melting of the bundles, and the systems (EKS) ceased to exist at $T_{L,L}$ [1]. Figure 1 is a reproduction of the 1975 thesis view on the morphology of amorphous polymers. The sketch represented the morphology which one could observe after etching the surface with a chemical reactant which would attack the interfaces (of lower density) first. The darker regions represent the interfaces.

At the present time (2019) the initial theory has been greatly modified and improved and, as a result, the presence of the bundles is not required to explain the stability of the EKS in terms of morphological structure, but the bb-balls and their interface made up of free bond-units are still present as discussed below.

2. The Search for a New Understanding of the b/F Coupling between Conformers: The Dual-Split Statistics

It is probably Flory who was *indirectly* responsible for a new interpretation of what I called in my thesis “the Energetic Kinetic Network Theory (EKNET)”. In a certain

sense, the 1975 thesis contradicted Flory's views on the amorphous state [5], and he was leading the opposition over the raging controversy on the presence of "local order" in the amorphous state of polymers. R.F. Boyer was at the other end of the spectrum, claiming evidence for local order. Then Flory won the Nobel Prize, almost immediately after Benoit [6] had confirmed by small angle neutron scattering (SANS) the total randomness of the macromolecules in the bulk. In the 1975 dissertation a morphological interpretation of the Energetic Kinetic principles was not necessary but was presented for convenience since, in order to have stable systems, it was convenient to find a morphological reason for this stability. This was the reason for creating the bundle as a special bb-ball (Figure 1). But, after the work of Benoit [6], it became unclear how, if there was actually no local order to stabilize the Energetic Kinetic Systems, the systems could become stable. *Could it be possible to have stable systems and no local order after all?*

The Dual-Split-Kinetic model, which provides the original set of equations for my understanding of the interactions between conformers to explain the presence of b and F conformers without local order, was conceived between 1976 and 1981. With this new proposed statistics of the conformers – see the next section – the local order concept was not needed to give life to the stability of the systems, and thus local order or "segment–segment melting", as it is now called [7], was not *required* to explain what I now see as a fundamental aspect of the interactive process between the conformers: the presence of the F and b dual-phase.

Hence, even if there are many similarities between the 1975 thesis version and the present presentation of polymer physics, there is also a fundamental difference which may be essential, not only because, obviously, it may provide a new light in polymer science, but also because it could also be generalized to other systems in interaction in physics, and provide a new angle to deal with delocalization and entanglement in particle physics. The essential difference with my thesis's presentation derives from the introduction of a dissipative term in the Dual-Split statistics describing the coupled states of the interactive conformers. This will be explained in the first chapter, a *preamble* to this book. The dissipative character of entanglements in polymers, for instance, will be shown to be the consequence of the Dual-Split Statistics of the conformers, leading to the Cross-Dual-Phase-Statistics. Likewise, the stability of entanglements in a melt could easily be coined in terms of a rheological temperature of a melt, located at or similar to $T_{L,L}$. It may be that Boyer was right in claiming strongly the existence of this upper transition but wrong in its interpretation as a local melting process. The confirmation of the existence of the $T_{L,L}$ transition might be strong experimental evidence of the existence of dual-phases, but not of local order. This is *not* to say that local order never exists for some polymers, especially for those which have a tendency to crystallize, but this is not the reason for $T_{L,L}$, although it can influence it. In this research strong evidence is offered suggesting that $T_{L,L}$ is associated with the sta-

bility of the Cross-Dual-Phase network, itself a function of the b/F Dual-Phase statistics.

3. The Search for a New Understanding of Flow Properties from the Conformers' Dual-Split Statistics ($M < M_e$) and Crossed-Dual-Phase Statistics ($M > M_e$)

This book is based on a compilation of several articles published in the *Journal of Macromolecular Science* over the last few years dedicated to the subject of melt deformation and flow of polymers. The link between the chapters is the new model used to describe the source of molecular motions and flow, which is the Dual-Split Statistics of the conformers; this model provides a quantitative way to determine stress and strain from the variation of the conformational state of the conformers. The Grain-Field Statistics, which generalizes the application of the Dual-Split Statistics of conformers to “open dissipative systems”, is responsible for the existence of “entanglements”, i.e. the split of the system of interactions between conformers into two open dissipative systems, which we call Cross-Dual Phases. This is the main originality of this work.

The eight chapters of the book concentrate in presenting the rheological results under this new view of the deformation of a network of interactive coupled dual-phase submitted to small or large deformations. Even without going into the mathematics of the Dual-Split Statistics or the Grain-Field Statistics, a separate subject on its own, the description of the linear and non-linear rheology of polymer melts from the perspective of a network of dual-phases at two interactive levels appears very simple and rich in potential applications. What is called “disentanglement”, for instance, can be described in the context of the stability of the network of Cross-Dual-Phases (Chapter 4). The industrial applications of “disentanglement” (and/or “shear-refinement”) are readily commercialized at the pilot stage: their large benefits are addressed in terms of energy savings during processing, throughput enhancement, mixing with thermally sensitive additives at low temperature, low degradation microinjection molding, and the manufacturing of new materials with enhanced physical properties (film permeability for the food packaging industry). Yet the lack of understanding of these achievements by the established models of flow (reptation) has impacted negatively the spread of this new technology, which has remained empirical and marginal, even looked down as “suspicious” by the reptation model followers...

The history of science is full of these stories of rejection of new ideas which stem from explaining new experiments apparently contradicting previously established concepts. In this book, we have taken the time to expose at length the experimental procedure and analyze the possible artifacts which could explain the results (Chapters 2–6). Yet one overwhelmingly convincing piece of evidence stands out, in our opinion: it is from the discovery of “sustained-orientation”, explained in Chapter 2, and studied in Chapter 4, that produces polymer granules

with properties that completely challenge the existing views in polymers. Not a single paper from the reptation school has addressed the issue of “sustained-orientation” since its first publication more than 5 years ago. We also present in Chapter 7 small angle neutron scattering (SANS) evidence that the established molecular dynamic models (e.g., reptation) misrepresent the deformation of a single macromolecular chain during shear-thinning, yet this is a basic, fundamental phenomenon of linear rheology. In Chapter 3, we carefully re-visit the basic concepts of linear rheology which have established dynamic molecular models as a trustworthy reference to study and explain flow in polymer melts. Our conclusions are somewhat at variance with those scientists who believe that the current established understanding of linear viscoelasticity is the jewelry of polymer science. On the contrary, we suggest that the concepts of relaxation times, local friction coefficient, time-temperature superposition temperature, and molecular weight between entanglement (M_e) may be limitations to understand flow under conditions of deformation used by the industry, i.e. at fast throughput (strain rate) and large strain.

In short, we have initiated and propose to use another molecular approach to describe the deformation process in polymer melts which encompasses small and large deformation without the difficulty inherent to the established dynamic models of flow, which are based on the description of the deformation of singular chains embedded in a mean field of interactions. In Chapter 4 it is shown that the strain induced time dependency of the rheological parameters (G' , G'') cannot be explained by reference to the reptation time alone and yet that non-linear viscoelastic deformation results can be understood and extrapolated from their linear (low strain) state if we assume the instability of the network of interactions that modulates the kinetics. In Chapter 5, we describe the physical parameters of the dual-phase rheology and the way to obtain them from experimental results. The important concept evolving from this new analysis is the existence and relative stability of the “network of entanglements”, which is expressed by the dynamics of the Crossed-Dual-Phases, giving rise to the elastic dissipative wave character of the melt. The elasticity of the network is, in this view, responsible for shear-thinning, whereas, at rest, without shear-deformation, the network dissipative properties explain the Newtonian behavior and also the solid-like characteristics of the melt which are studied in Chapter 6. The orientation of the entanglement network, generated by the anisotropy of the blinking deformation process at large frequency (or amplitude) explains the rubbery plateau region in a totally different way than the established models.

I have designated the presentation of these new views about interactions in polymer chains and their entanglement “New School of Polymer Physics” and suggest that it may represent a paradigm shift which will inspire the development of new concepts in physics and new innovative products and processes in engineering.

References

- [1] Ibar, J.P., *A New Theory For the Properties and the Behavior of Polymeric Materials*, PhD thesis, M.I.T (1975), unpublished: <https://sites.google.com/a/eknetcampus.com/dual-split-statistics/>
- [2] Volkenstein, M.V., *Dokl. Akad. Nauk SSSR* (1951) 78, p. 879.
- [3] Robertson, R.E., in “*Structure and Mobility in Molecular and Atomic Glasses*”, *Ann. N. Y. Acad. Sci.*, Vol. 371, O’Reilly, J.M., Goldstein, M., Eds.; New York Academy of Sciences (1981), pp. 21–37
- [4] Robertson, R.E., *J. Chem. Phys.* (1966) 44, p. 3950
- [5] Williams, A.D., Flory, P.J., *J. Polym. Sci.* (1968) C16, p. 2981
- [6] Benoit, H., *Polymer Preprints*, (1974) 15, 2, p. 324.
- [7] Boyer, R.F., in “*Computational Modeling of Polymers*”, Bicerano, J., Ed., Marcel Dekker, New York, (1992), pp. 1–52.

Contents

Acknowledgments	VII
Preface	IX
Chapter Abstracts	XVII
1 Preamble	1
1.1 Introduction	1
1.1.1 The Classical View of Polymer Visco-elasticity, Shear-Thinning, and Entanglements	2
1.1.2 The Dual-Split Statistics View of Polymer Visco-elasticity, Shear-Thinning, and Entanglements	3
1.2 Introduction to the Dual-Phase Model of Polymer Interactions and to the Cross-Dual-Phase Model of Entanglements	4
1.2.1 A New Model of Polymer Interactions (Summary)	4
1.2.1.1 Conformers: The b and F Types of Conformers	6
1.2.1.2 The Dual-Split Statistics of the Conformers: [b/F \leftrightarrow (c,g,t)]	8
1.2.1.3 Crossed Dual-Phase Statistics for Long Chains	13
1.2.2 A New Understanding of Polymer Melt Molecular Interactions and Flow Properties	15
2 Trouble with Polymer Physics: “Sustained-Orientation”: Ground-Breaking Experimental Research Shakes the Current Understanding of the Liquid State of Polymers	21
2.1 Introduction	21
2.2 Experimental Description	22
2.2.1 The Rheo-Fluidification Processor	22
2.2.2 Sustained-Orientation	23
2.3 Results	25
2.4 Discussion	27

2.5	Summary and Conclusions	29
2.6	Note	29
3	The Great Myths of Polymer Rheology: Comparison of Theory with Experimental Data	31
3.1	Introduction	32
3.2	Shear-Thinning: Non-Newtonian Viscous Behavior	34
3.3	Description of the Data Sources	36
3.4	Analysis Protocol	40
3.5	Accuracy Consideration	40
3.6	Critical Analysis of the Equations of Rheology	44
3.6.1	Universality of WLF Constants at T_g	44
3.6.2	Validity of the 3.4 Power Exponent for $M > M_c$	48
3.6.3	For $M < M_c$, Viscosity Is Not Proportional to M , Contrary to Rouse's Model	52
3.6.4	Accuracy in the Determination of the Newtonian Viscosity	54
3.6.5	Time-Temperature Superposition	59
3.6.6	The Upper Melt Temperature Departure from Superposition	63
3.6.7	The Lower Melt Temperature Departure from Superposition	67
3.6.8	Is the Superposition Principle Ever Valid?	71
3.7	The Question of Understanding Rheology with a Spectrum of Relaxation	73
3.8	Conclusions	85
4	The Great Myths of Polymer Rheology: Transient and Steady State. The Question of Melt Entanglement Stability	89
4.1	Introduction	89
4.1.1	Transient and Steady State Behavior	89
4.1.2	Step Strain Experiment in the Non-linear Region	90
4.1.3	Step Strain Rate Experiments under Non-linear Conditions	94
4.1.4	Strain-Induced Transients under Oscillatory Shear	96
4.1.5	Combining Rotation and Oscillation Shear Modes	98
4.1.5.1	The Work of Osaki et al.	98
4.1.5.2	Effect of Combining Rotation and Oscillation in the Non-linear Regime: Shear-Refinement under Dynamic Conditions	100
4.1.6	Melt Fracture. Edge Fracture in Parallel Plate Experiments	113
4.1.7	Objectives of This Chapter	114

4.2	Experimental Procedure, Polymer Characterization, Definition of Parameters	116
4.2.1	Experimental Procedures	116
4.2.1.1	Type 1A: The Simple Time Sweep at Given T , ω , and Strain	116
4.2.1.2	Type 1B: The Simple Time Sweep at Given T , ω , and Strain % Immediately Followed by a Cooling Ramp Test Performed in the Linear Range	116
4.2.1.3	Type 2: The Three-Step Experiment of Type FTF (Frequency–Time–Frequency) in a Dynamic Rheometer	117
4.2.1.4	Type 3: The Four-Step Experiment of Type FT1–FT2–FT1–FT2 in a Dynamic Rheometer	117
4.2.1.5	Type 4: Pure Viscometry	117
4.2.1.6	Type 5: Pure Viscometry Followed by a Frequency Sweep	117
4.2.1.7	Type 6: Viscosity Measurement under Extrusion Flow Conditions	118
4.2.1.8	Type 7: In-line Viscosity Measurement at the End of a “Treatment Processor”	118
4.2.2	Rheometers Used	118
4.2.3	Materials	119
4.2.4	Initial State and Sample Molding Procedure	121
4.2.5	Definition of the Rheological Parameters to Analyze the Stability of the Melt	122
4.3	Results	127
4.3.1	Linear PC (Lexan 141). Time Sweeps at Various Temperatures, Frequencies, 50% Strain	127
4.3.2	Viscosimetric Experiments on LLDPE	130
4.3.2.1	Pure Rotation. Type 4 Experiment	130
4.3.2.2	Pure Rotation Followed by Frequency Sweep. Type 5 Experiments	142
4.3.2.3	Type 4 Experiments on Melts with Prior Mechanical History	146
4.3.2.4	Transients Created in Dynamic Conditions by an Increase of Strain	150
4.3.3	Dynamic Type 2 Experiments (FS–TS–FS) on PC	153
4.3.3.1	Effect of Strain at Constant Low Frequency (0.1 Hz)	153
4.3.3.2	Effect of Frequency during Time Sweep (at a Constant Strain of 5%)	173
4.3.3.3	Effect of Increased Energy Input during Time Sweep: $T = 225\text{ }^{\circ}\text{C}$, Frequency = 5 Hz, and $\gamma = 20\%$	185
4.3.3.4	Effect of Annealing the Melt after Treatment and Type 3 Experiments	191

4.3.4	Long-Term Entanglement Network Instability for a PMMA Melt	199
4.3.5	Entanglement Network Instability for a Polystyrene Melt	202
4.3.5.1	PS 1070	202
4.3.5.2	PS2: Thermal–mechanical History to Create Out-of-Equilibrium Melt Properties	206
4.4	Discussion	210
4.4.1	The Question of the Origin of the Time Dependency of the Viscoelastic Parameters	210
4.4.2	Challenging Interpretations	211
4.4.2.1	Viscous Heating	211
4.4.2.2	Shear Degradation	211
4.4.2.3	Drooling of the Melt Outside the Rheometer Plates	213
4.4.2.4	Plastification Due to an Increase of the Monomer Concentration by the Shear Process	215
4.4.2.5	Shear-Thinning	216
4.4.2.6	Edge Fracture Explanation	216
4.5	Summary	249
4.6	Conclusion	250
5	The Great Myths of Polymer Rheology: Elasticity of the Network of Entanglements	257
5.1	Background	257
5.2	Introduction	259
5.3	The Cross-Dual-Phase Network of Entanglement	264
5.4	The Static and Dynamic Frequency of the Phase-Wave	265
5.5	The Influence of $T_g(\omega, \gamma)$ on the Rheology Data	280
5.6	The Cohesive Network Energy	292
5.7	Effect of Temperature	296
5.7.1	T Ramp Down Experiments	296
5.7.2	Frequency Sweeps at T Constant	301
5.7.3	Diversity of the Temperature Dependence Depending on the Polymer Type	313
5.8	Effect of Strain %	322
5.9	The Melt Behavior at Low Frequency	359
5.10	Summary and Conclusions	365

6	The Elastic Dissipative State of Polymeric Melts. Solid-like Behavior in the Molten State	385
6.1	Introduction	385
6.2	Noirez et al. Solid-like Results	388
6.3	Why Narrowing the Gap Makes χ_1 Increase (The Melt Is More “Glassy-like”)	397
6.4	Is There a Surface Effect in the Experiments Reported by Noirez et al.?	398
6.5	The Question of the Nature of the Elasticity in the Solid-like Melt	400
6.6	Conclusion	401
7	Shear-Thinning of Polymeric Melts: The Failure of the Reptation Model	403
7.1	Rheo-SANS Results of Watanabe et al. (2007)	403
7.2	Rheo-SANS Results of Noirez et al. (2009)	404
7.3	New Rheo-SANS Evidence by Zhe Wang et al.: “Fingerprinting Molecular Relaxation in Deformed Polymers”	405
7.4	Discussion and Conclusions	409
8	Conclusions – Entanglements: A New Interpretation and Perspectives in Science and Technology	417
8.1	Summary of the Book’s Previous Chapters	417
8.2	Industrial Applications: Improve the Processability of Existing and New Resins	419
8.3	A New Paradigm: Future Achievements	422
8.4	Appendix A	426
	Index	427

1

Preamble

1.1 Introduction

Viscosity represents the resistance to flow. It describes how the constituents of a liquid interact to respond to a mechanical deformation, in this preamble, a shear deformation imposed dynamically to polymer melts with radial frequency ω . At vanishing strain rate (or frequency $\omega \rightarrow 0$), the stress required to shear the melt vanishes to zero, but the ratio of stress to strain rate is finite: this is the Newtonian viscosity, a parameter that expresses the pure viscous character of the state of interactions between the macromolecules. Shear-thinning behavior (also called “pseudo-plasticity” behavior), describes the fact that viscosity decreases as the strain rate (or ω) increases. The melt is then designated as non-Newtonian. Figure 1.1 illustrates the phenomenon of shear-thinning.

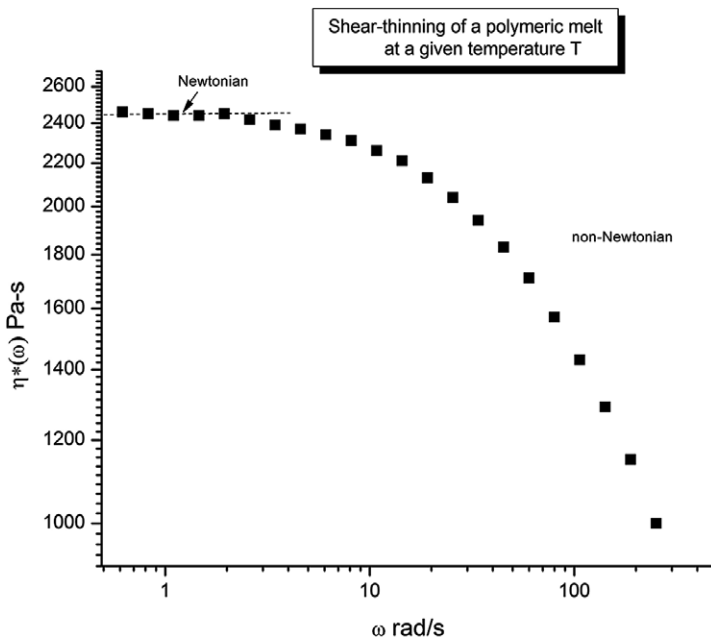


Figure 1.1 Viscosity vs frequency (log-log) illustrating the concept of Newtonian and non-Newtonian viscosity (shear-thinning)

1.1.1 The Classical View of Polymer Visco-elasticity, Shear-Thinning, and Entanglements

Classical visco-elasticity theory [2, 3] considers shear-thinning of a polymer melt as a disturbance by the flow rate of the pure liquid state – described by the Newtonian viscosity – due to the orientation of the chains by the stress field. “This reduction of viscosity is due to molecular alignments and disentanglements of the long polymer chains”, claim Vlachopoulos and Strutt [4]. The well-known Carreau’s formulation of the strain rate dependence of shear viscosity [5] correctly describes the relationship, from low to high ω , which translates this concept of a state variable, the Newtonian viscosity, continuously modified by a factor controlled by the degree of orientation of the singular macromolecular chains, which itself is a function of strain rate (ω). The concept of relaxation time, τ , and its correlation to the internal friction, thus to the viscosity, permits us to transcribe the dynamic shear viscosity η^* in molecular (effect of M) and topological (M/M_e) terms, where M is the molecular weight of the chain and M_e the critical molecular weight between entanglements. In the claimed molecular interpretations of shear-thinning [6–8], these parameters and the introduction of a characteristic relaxation time, called the reptation time, determine the dynamics of the melt, i.e., the effect of strain rate on viscosity and modulus. In de Gennes’s molecular interpretation of the viscosity results [6], the deformation of single chains is the focus of attention. The macromolecular chain is embedded in a field of interactions created by the other chains that confine its motion within a tube in which it can reptate; the process is governed by the reptation time. For polymer melts, a single relaxation time does not explain all the visco-elastic results in the linear regime (at low strain), yet a spectrum of relaxation times does, which can be derived from the properties of the reptation time and its dependence on temperature and molecular weight [2, 3, 6–8].

Doi and Edwards [8] attribute the departure from non-Newtonian behavior to the reptation time, τ_d , of the de Gennes theory, which they determine experimentally at the cross-over frequency, ω_c , of $G'(\omega)$ and $G''(\omega)$: $\tau_d = 1/\omega_c$. When the melt is sheared in the terminal region, shear-thinning is due to the orientation of the macromolecule segments in the direction of the stress gradient. Shear-thinning occurs when the strain rate surpasses the reciprocal of the reptation time; the viscosity continues to decrease as strain rate increases until the rubbery plateau region is reached, which occurs at the minimum of $\tan \delta$, where δ is the phase difference between stress and strain, a characteristic of the visco-elastic nature of the melt. The phase difference is 90° for a pure viscous liquid (Newtonian), 0 for a pure elastic solid and is at its minimum at the onset of the rubbery plateau, allowing us to characterize the entanglement density and the rubbery plateau modulus $G_{0,N}$. For instance, for polycarbonate, $M_e = 2500$ g/mole and $G_{0,N} = 1.5$ MPa [9].

The Newtonian viscosity, η^*_0 , only depends on temperature, and has been correlated to the amount of free volume present in the melt. This was discovered for small liquids by Doolittle [10] and further applied to polymers by William, Landel, and Ferry, authors of the famous WLF equation [3]. The molecular weight dependence of η^*_0 is derived from the variation of the reptation time with M , which scales like $M^{3.4}$.

In summary, classical visco-elasticity theory explains the melt deformation with one mechanism of deformation, the chains being stretched, their rms end-to-end distance increasing, and with the possibility of slips of the entanglement points that determine the network structure. Chapter 3 will provide an overview of the predictions, successes, and shortcomings of the classical model of visco-elasticity. This can also be found in Ref. [11].

1.1.2 The Dual-Split Statistics View of Polymer Visco-elasticity, Shear-Thinning, and Entanglements

On the other hand, the Dual-Phase visco-elastic model, presented in Refs. [12] and [13], suggests a very different origin for shear-thinning, strain softening, and entanglements. It actually projects the possibility to obtain various Newtonian viscosity values at a given temperature by bringing the melt out of equilibrium by processing it by Rheo-Fluidification [14, 15]. This model is briefly presented in the next section.

For the sake of clarity when reading this book, it appears useful to present early on a short review of the concepts that led to the anticipation of the experimental results addressed below.

In the classical view, the chain is particularized and its interaction with its surroundings is described in terms of a mean field of interactions. The entropy of a single chain is calculated from its intra-molecularly linked covalent bonds and the deformation (to express flow properties, for instance) is due to a modification of the entropy. The presence of the other chains is perceived as a restriction on the entropy (in particular, in de Gennes's well-praised model [6, 7]) by the confinement of the motion of the chain within a tube in which the chain can reptate. The sophistication of the "reptation" model comes from the refinement of the definition of the tube itself [8, 16–19].

In this preamble, we summarize our new way to describe the complexity of the interactions between polymer macromolecules, in particular a new way to determine the conformational state of the basic constituents of the macromolecules, the conformers, which are covalently bound to each other along the chains, yet exert inter-molecular forces with adjacent conformers belonging to the same or to other macromolecules.

■ 1.2 Introduction to the Dual-Phase Model of Polymer Interactions and to the Cross-Dual-Phase Model of Entanglements

1.2.1 A New Model of Polymer Interactions (Summary)

A macromolecule can be viewed as a succession of real or virtual three-bond elements, which we call “conformers”. For simple macromolecules (polyvinyl chloride, polyethylene, polytetrafluoroethylene, polystyrene, polyacrylates, etc., and most of the polyvinyls), the macromolecule can be described with a succession of three-bond elements, as presented in Figure 1.2. For these simple systems, the length of the conformer C_1C_2 , C_2C_3 , C_3C_4 corresponds to the length of three covalent bonds of the repeating unit.

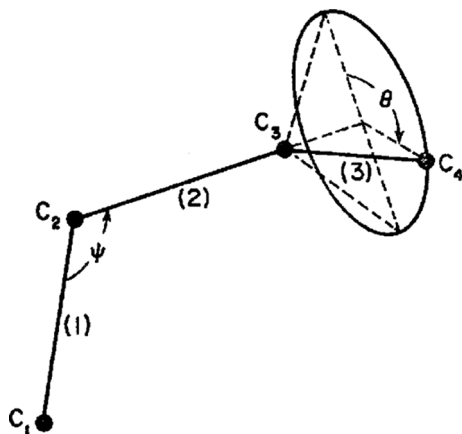


Figure 1.2 Conformer

For other systems, the situation is slightly more complex and the length of the bonds of the repeating unit is not the length of C_1C_2 , C_2C_3 , C_3C_4 of the “virtual three-bond element”. A good example is given in Figure 1.3 and Figure 1.4 for polycarbonate of bisphenol-A, the polymer studied in many chapters of this book.

Champetier and Monnerie [20] and Lunn [21] reported the work of several authors [27] who studied the statistical shape of the random chain in dilute solution, i.e., the chain conformation less affected by inter-molecular forces, and concluded that the carbonate group $O-CO-O$ was planar (stabilized by electron resonance over the three oxygen atoms) and that the “trans” form of the carbonate group was preferred over the “cis” (see Figure 1.3(a) and (b)). An infra-red spectroscopic study of polycarbonate [21] led to the conclusion that the planes of adjacent benzene rings

nature of the bond interactions (Figure 1.8 and Figure 1.9). So, in fact, there are two interactive layers of duality, which is the reason we use the expression cross-dual-phase to describe the entanglement network. In other words, the solution to the coupled dual-phase statistics of the interpenetrating macro-coils, which we call the Grain Field Statistics, does not define four phases but two dual-phases, like two types of crystallographic structures co-existing interactively. Melt cohesion implies a fluctuation of the channel/core phase contours, which are constantly in motion, like froth in an agitated sea near the shore (Figure 1.11). The characteristics of this cross-dual-phase “entanglement network” are governed by the molecular weight of the macro-coils as well as the properties of the conformers $[b/F \leftrightarrow (c,g,t)]$ described by the dual-phase statistics discussed earlier. The interpenetration of the macro-coils disturbs the dual-phase statistics, which splits into two coherent and interactive phases, creating the river network sketched in Figure 1.11. To simplify, we call the white fluctuating strands in Figure 1.11 the “entanglement phase”; we also use the expression “phase-lines”.



Figure 1.11 Sketch of the Cross-Dual-Phase entanglement network model. The boundaries of the “white phase” are not static but fluctuating around with frequency ω'_0 under no stress conditions. Stress increases the frequency of reorganization and, in the rubbery plateau region, preferentially orients the boundaries in the flow direction. This can be modeled by an activated process

1.2.2 A New Understanding of Polymer Melt Molecular Interactions and Flow Properties

As a general statement, the problem of melt deformation consists of determining how the Cross-Dual-Phase network can produce strain coherently, from the local re-organization of the local conformers in one dual-phase or in each phase, to the orientation with the stress of the entanglement phase, resulting in the orientation of the network of entanglement. As described in detail in another publication [12],

■ 2.2 Experimental Description

2.2.1 The Rheo-Fluidification Processor

In a Rheo-Fluidification processor, a melt extrudes continuously through treatment zones where it is submitted to a combination of shear-thinning and strain-softening via the use of cross-lateral shear vibration superposed to pressure flow (originated by an extruder feed). Figure 2.1 shows two treatment stations – (11) and (22) – for a melt flowing from left to right to exit at the end of the processor, where its viscosity is measured continuously by an in-line rheometer and it is water cooled, granulated into pellets.

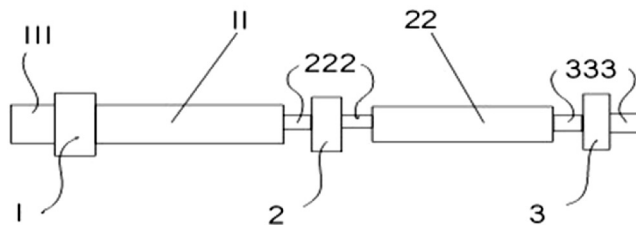


Figure 2.1 Schematic of a Rheo-Fluidizer with two stations

The “treatment” in stations (11) and (22) is sketched in Figure 2.2: the melt flows through (from left to right) a gap, “3”, where the upper gap surface is static and the lower surface is rotated and (optionally) oscillated. Both surfaces contain small ribs, “12”, detailed in Figure 2.3 and Figure 2.4, which create local vibrational extensional flow by squeezing and un-squeezing the melt as it is being swept forward helicoidally.

Shear-thinning is controlled by the shear rates, which add up vectorially from all types of flow (longitudinal and cross-lateral, vibratory or not), and strain softening is controlled by frequency and the strain amplitude of the cross-lateral shear component. The rotation of the rotor in station 1 and station 2 were in opposite directions, a situation that we casually called “comb to the left–comb to the right”, referring to the sweeping induced by the ribs in relation to the rotation direction.

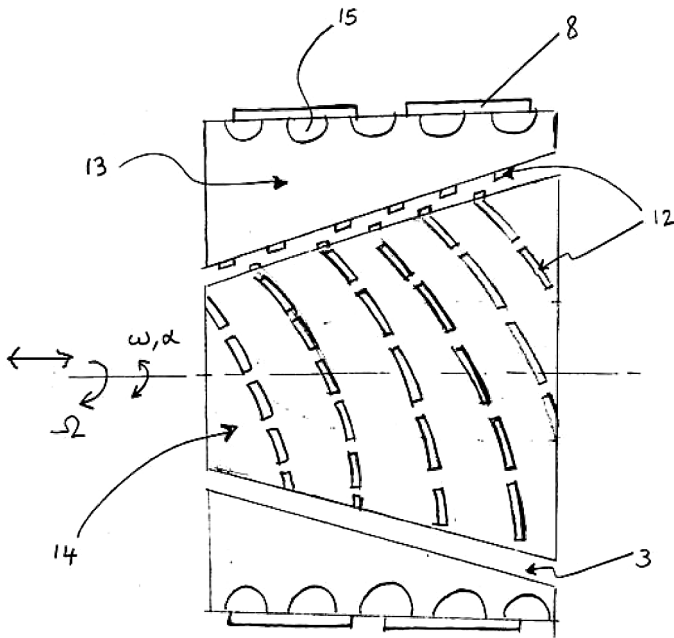


Figure 2.2 Details of the “inside” of one station in Figure 2.1

2.2.2 Sustained-Orientation

Figure 2.5 shows the viscosity of the exiting melt (PMMA) just after it has been “treated”, i.e., at the end of the second station of the two-station Rheo-Fluidizer shown in Figure 2.1.

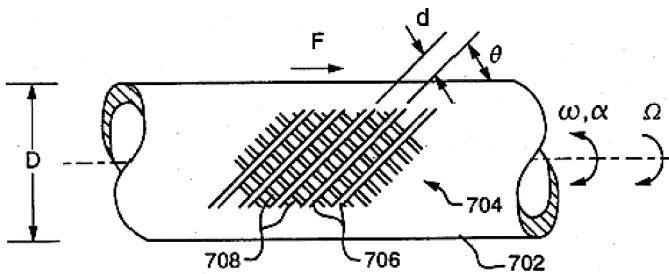


Figure 2.3 The surfaces touching the melt have a network of “ribs” to induce vibration as the melt passes through

perature, frequency sweep tests show a gradual return to a normal pseudo-plasticity and Newtonian viscosity.

Table 2.1 Flow Improvement for Pellets Showing Sustained Orientation

	Virgin MFI	MFI after “treatment” (and correction for M_w change)	Flow improvement (%)
Polycarbonate	12	21	75
PETG	8	12	50
LLDPE	0.5	1.2	140
Polystyrene	4	6	50
PMMA	17	37	118

■ 2.4 Discussion

Our research has two goals: (1) a theoretical, fundamental understanding of the stability of the network of entanglement and (2) a practical goal: how Rheo-Fluidification proceeds by way of “disentanglement of the chains”, and how we can predict the processing parameters responsible for its triggering (temperature, strain, strain rate in both shear and extension) that will produce sustained-orientation. The theoretical objective raises fundamental questions regarding our present understanding of the interactions between the macromolecules that give rise to entanglements, these “physical cross-links”. Our experiments at least suggest that the classical concept of M_e to describe entanglements is too simplistic and its usefulness is probably limited to the linear range of viscoelasticity.

The practical goal of this program will be fully achieved when we will be able to predict the processing parameters for a successful Rheo-Fluidification treatment, yielding any chosen value of sustained-orientation, given a polymer melt of known molecular weight characteristics, topology, and chemical structure. In simple terms, for a given throughput of melt flow, what should be the Rheo-Fluidification processing temperatures in the stations, the value of combined strain rate (from pressure and drag flow, oscillatory and rotational), the value of extensional flow and strain rate, the value of pressure in the gap, and what will be the amount of sustained-orientation obtained? Further, what will be the stability of the new entangled state (how fast will it re-entangle at any given temperature and pressure)? Therefore, the theoretical and fundamental part of this research is to provide a science base for molding processes under shear-thinning and strain-softening controls, so that the process result can be achieved rationally based on scientific laws rather than only on experience.

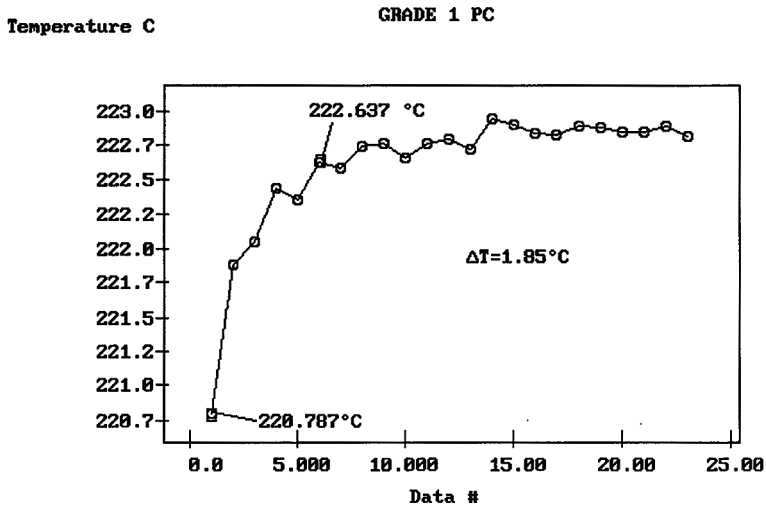


Figure 3.8 Stabilization of temperature in the rheometer oven as a function of the data point measurement (corresponding to a frequency increase). The increase of temperature of 1.85 °C corresponds to the sixth data point

In summary, it seems appropriate to warn against the use of “uncontrolled” data from various sources to test the validity of sensitive equations. “Randomness” of the residuals for alleged good fits might be artificially created by mixing data from several workers, and mistaken with the effect of thermal history, which is known to create scatter and an unacceptable level of accuracy compared to experimental errors. As already said before, it seems more appropriate to generate the data carefully, using the same protocol of sample preparation, the same procedure to test the specimen, the same instrument to determine molecular weight characteristics, the same instrument to measure the viscoelastic data, by the same operator, and especially using the same lot for the resin.

■ 3.6 Critical Analysis of the Equations of Rheology

3.6.1 Universality of WLF Constants at T_g

The simplest myth to knock down, because it is already largely admitted, is the myth that universal constants C_{1g} and C_{2g} enter the WLF formulation of Newtonian viscosity, Eq. (3.3).

Figure 3.9 is a plot of $\text{Log}(\mu_o/\mu_{og})$ vs $(T - T_g)$ for the three polycarbonate grades. The value of T_g for the respective polymers is known from PVT analysis, by inter-

cepting the rubbery and glassy volume-temperature behavior, at atmospheric pressure. The Newtonian viscosity μ_o at each temperature is obtained by fitting the non-linear behavior with the generalized Cross-Carreau equation, Eq. (3.6). For each grade, we verify that $\text{Log}(\mu_o)$ vs T can be fitted rather well (with r^2 better than 0.999) by a hyperbolic function, which can, indeed, be rewritten as a WLF equation, Eq. (3.3) [17], from which the two constants C_{1g} and C_{2g} are derived. The value of μ_{og} in Figure 3.9 and Eq. (3.3) is computed by extrapolation from the hyperbolic fit, knowing the value of T_g (see Table 3.1).

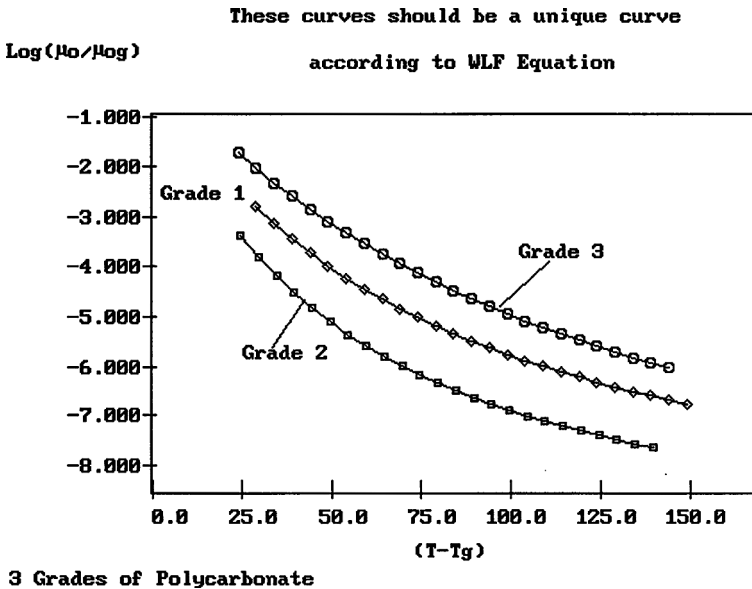


Figure 3.9 $\text{Log}(\mu_o/\mu_{og})$ vs $(T - T_g)$ for PC. These three curves should be a single curve according to the WLF equation

Table 3.1 Fitting Parameters in WLF Eq. (3.3) for the Three PC Grades of Figure 3.9

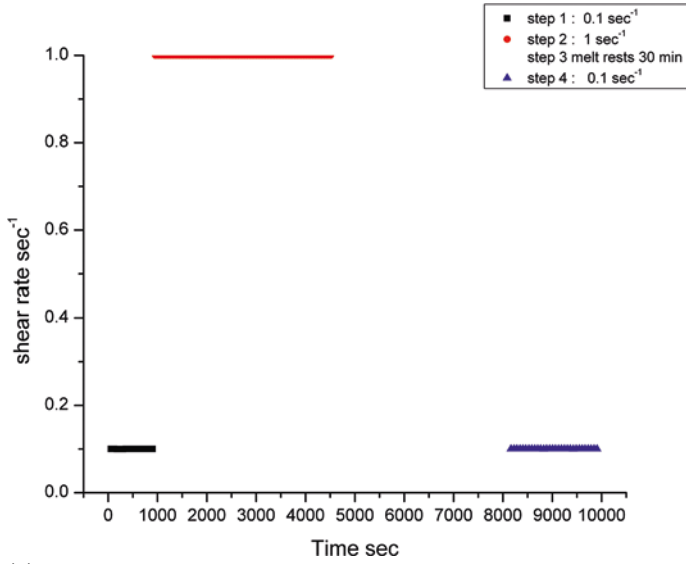
	T_g ($^{\circ}\text{C}$)	$\text{Log}(\mu_{og})$	C_{1g}	C_{2g}
GRADE 1	136.0	9.842	10.22	76.70
GRADE 2	145.4	11.58	10.46	51.88
GRADE 3	151.0	12.06	11.87	84.16

Figure 3.9 demonstrates that plots of $\text{Log}(\mu_o/\mu_{og})$ vs $(T - T_g)$ for the three polycarbonate grades do not resume to a single curve, as predicted if the WLF constants were universal [17]. The values obtained for C_{1g} and C_{2g} are convincingly different from the universal constants proposed by William, Landel, and Ferry [17], respectively 17.44 and 51.6. Also, it is observed that $\text{Log}(\mu_{og})$ for the three grades is not equal to 13, and does not stay constant with molecular weight, even for the two linear polymers Grade 1 and 2.

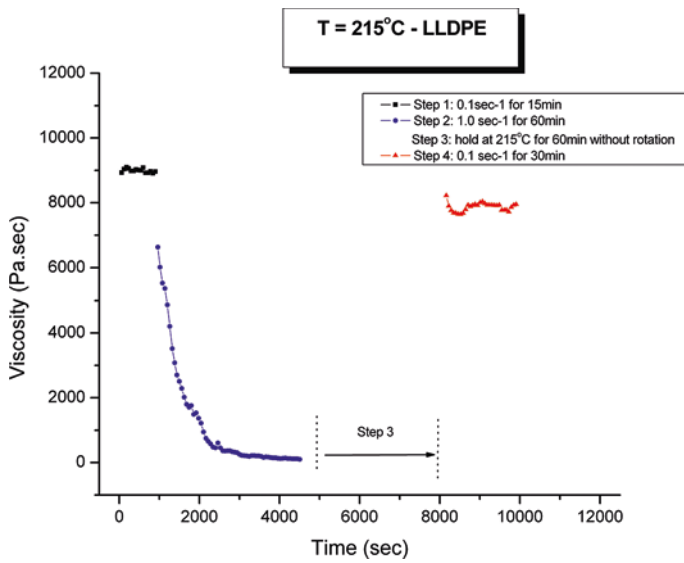
Thus, based on the second conclusion, a melt can have several steady states at the same temperature and strain rate, depending on its state of entanglement, and it appears that shear can modify the entanglement state at will: this is the basis of “shear-refinement”. If entanglements can be kept in an unstable state long enough, it is possible to produce “disentangled polymers” that, in terms of viscosity decrease, are attractive commercial “grades”. The challenging question is how to retain in a metastable state (that we could control) the lower viscosity melt produced at the end of a transient “treatment” and then recover the original properties after processing.

Another conclusion seems to emerge from these experiments: shear-thinning might just become time dependent, under certain strain rate conditions. In other words, whatever causes shear-thinning produces a melt state that is not stable under certain conditions. The transient behavior observed would be the reflection of that time dependence of shear-thinning, and the molecular motions involved in shear-thinning and in the transient decay might be closely related, if not identical.

Figure 4.20 shows the effect of annealing the melt in the middle of a transient decay to see if the melt would reconstruct its internal structure to provide the original viscosity after annealing. The shear rate history shown in the box of Figure 4.20a was applied to the melt (the temperature was 215 °C). The difference with Figure 4.18 is that the melt was rested (un-sheared) for 30 minutes at the end of the transient decay induced by a shear rate of 1 sec⁻¹. Then the melt was sheared at a rate of 0.1 sec⁻¹. Figure 4.20b shows the variation of viscosity with time, Figure 4.20c shows the variation of normal force, and Figure 4.20d presents details of (c) around the zero normal force line. It is clear (Figure 4.20b) that the melt nearly regained its original viscosity after the time of rest when no mechanical deformation was applied. This is evidence that the equilibrium state for a strain rate of 0.1 sec⁻¹ was the original viscosity. The normal force was almost zero for the initial strain rate (Figure 4.20c, left curve), went up, and decayed when the strain rate was changed to 1 sec⁻¹, and was zero for the second application of a 0.1 sec⁻¹ strain rate. Zooming in on the zero line region of box (c) shows that the normal force decay during transient behavior actually converged to a small negative value (step 2 curve), but that after annealing (step 4 curve), the normal force had returned to zero.



(a)



(b)

scribe the data well enough to determine ω'_o accurately. There are other empirical functions, such as a Carreau type of equation, Eq. (5.2), which could be applied to describe the relationship between ω' and ω equally well within the range of ω . Figure 5.12 demonstrates another way to find ω'_o that, in our opinion, has much more physical significance, as will be shown later. This figure shows that ω' can be expressed as a function of G^* and that it could be fitted (for small strain) by a simple exponential growth function:

$$\omega' = \omega'_o + A_1 \cdot [\exp(G^*/G_1^*) - 1] \quad (5.12)$$

Here, in Figure 5.12, $\omega'_o = 34.1$; $A_1 = 58.733$; $G_1^* = 0.0279$ MPa. Eq. (5.12) can be rewritten as:

$$\begin{aligned} \text{Ln} \left(\frac{k\omega' + (1-k)\omega'_o}{\omega'_o} \right) &= \frac{G^*}{G_1^*} \\ \text{with} \quad k &= \frac{\omega'_o}{A_1} \end{aligned} \quad (5.13)$$

In this form, a mixing formula between ω' and ω'_o appears in the numerator of the logarithm, with compounding factor k . One can define an average ω'_{av} equal to $(k\omega' + (1-k)\omega'_o)$, with k constant in the regime of deformation described in Figure 5.12 (we will see later that k is a strong function of the strain γ). In the section dealing with the effect of strain, we identify k with the activated phase-lines coherence factor for a given ω' , the $(1-k)$ non-activated (or relaxed) ones having the static frequency ω'_o . This concept that the phase-lines of the entanglement network in Figure 5.7 do not need to be strained all at once, nor all the time, implies a sequential stretch-relax mechanism, and in that sense, k can be regarded as the fraction of time an activated phase-line is stretched (with ω' a frequency defining the stretched state), while $(1-k)$ is the fraction of time it is in the static, unstressed state (characterized by ω'_o). A similar mixing rule formula will be described in a later section giving a description of shear-thinning from the point of view of the cohesive energy of the network.

When $k = 1$ in Eq. (5.13), the formula simplifies to the classical Eyring modelization of flow, Eq. (5.14), in which stress “plasticizes” the activation energy of diffusion, which we find from the temperature variation of ω'_o (see next section):

$$\begin{aligned} \omega'_o &= \omega'_{oo} \exp \left(-\frac{\Delta\omega'}{RT} \right) \\ \omega' &= \omega'_{oo} \exp \left[-\frac{\left(\Delta\omega' - \left(\frac{RT}{G_1^*} \right) G^* \right)}{RT} \right] \end{aligned} \quad (5.14)$$

where $\Delta_{\omega'}$ is the activation energy for the diffusion of the static phase-wave, T is absolute temperature, R is the gas constant, and ω'_{00} is the frequency of fluctuation at absolute zero temperature (which should match the frequency of the conformer motions at $T = 0$ K). The ratio (RT/G^*_1) appearing in front of the modulus can be re-written by re-plotting the data in Figure 5.12 as a function of stress, instead of modulus, to conform to what the Eyring formula stipulates. The modulus G^* is equal to τ^*/γ where τ^* is the shear stress amplitude; so, if we plug this expression into Eq. (5.13), we now obtain $(RT/G^*_1\gamma)$ for the stress coefficient in Eq. (5.14). For instance, for the PMMA of Figure 5.12, obtained from a frequency sweep done at 2% strain: $\omega'_0 = 34.1$, $k = 0.5807$, $(T/G^*_1) = 0.01803$, and thus $(T/G^*_1\gamma) \sim 1$. This gives an order of magnitude for the stress coefficient in Eq. (5.13).

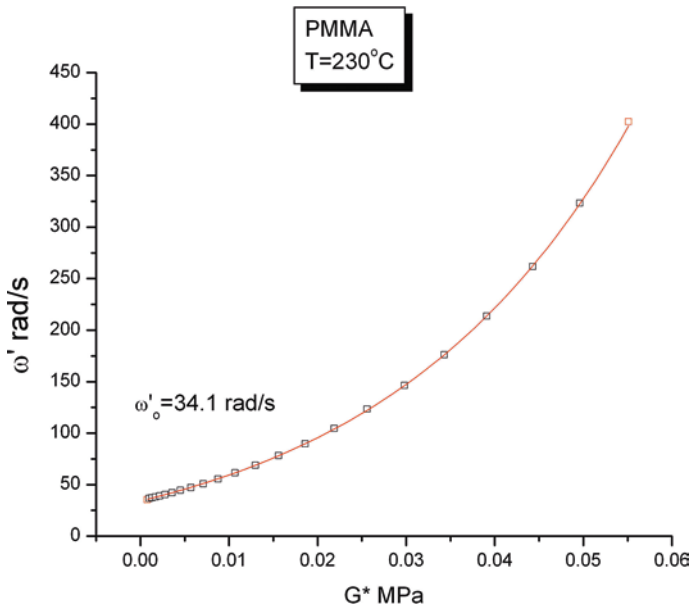


Figure 5.12 Plot of ω' vs G^* for PMMA at $T = 230$ °C, 2% strain. ω'_0 is found by extrapolation to $G^* = 0$. The continuous line is a fit by Eq. (5.12)

When k is different from 1, we can apply the same rewrite of Eq. (5.13) into the Eyring format but using ω'_{av} instead of ω' . We obtain:

$$\omega'_o = \omega'_{oo} \exp\left(-\frac{\Delta_{\omega'}}{RT}\right)$$

$$\omega'_{av} = \omega'_{oo} \exp\left[-\frac{\left(\Delta_{\omega'} - \left(\frac{RT}{G^*_1\gamma}\right)\tau^*\right)}{RT}\right]$$

$$\omega'_{av} = k\omega' + (1 - k)\omega'_o \quad (5.15)$$

In Figure 5.96, we see the split of $(G'/G^*)^2$ vs ω for a PS melt that has been submitted to a certain thermo-mechanical history prior to performing the frequency sweep done at 217.5 °C, with a strain of 30%. The frequency increases during the test, an option usually designated “an upsweep”.

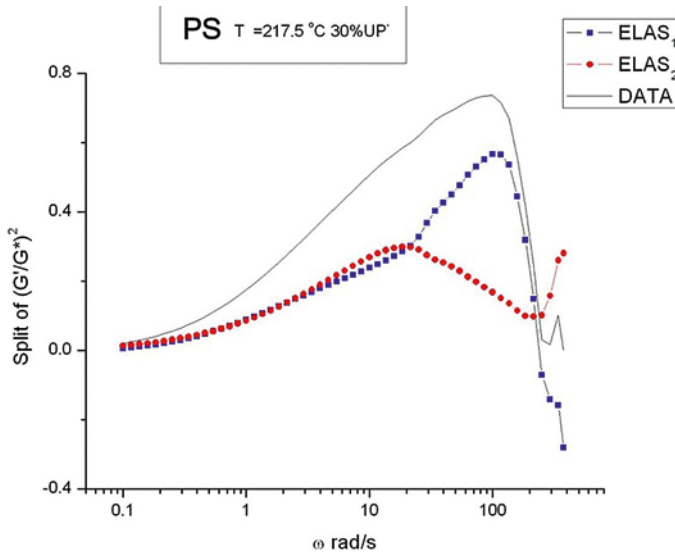


Figure 5.96 Split of $(G'/G^*)^2$ vs ω into χ_1 and χ_2 for the PS melt at $T = 217.5$ °C and $\gamma = 30\%$

In the legend box, $ELAS_1$ and $ELAS_2$ represent χ_1 and χ_2 , respectively. The $(G'/G^*)^2$ curve is also shown in the figure (“DATA”). One sees for this pre-sheared melt that both χ_1 and χ_2 rise simultaneously with ω and that χ_2 reaches a maximum at $\omega \sim 20$ rad/s while χ_1 continues to rise, yet χ_1 itself reaches a maximum at $\omega = 100$ rad/s before rapidly decreasing. The maxima for χ_2 and χ_1 are 0.3 and 0.6, respectively. It is interesting to see the large impact of a pre-shearing treatment of the melt (a condition called “shear-refinement”) on the modification of the rheology of the dual-phases; an untreated PS melt behaves very closely to what we have analyzed for PMMA (see Figure 5.81 and Figure 5.91). The new method of analysis of viscoelastic data presented in this chapter appears quite powerful to determine what happens to shear-thinning or strain softening as a result of a given shear-refinement treatment. In Figure 5.96, from $\omega = 0.1$ to 20 rad/s, the two dual-phases are in the terminal zone, both shear-thinning incoherently. Between $\omega = 20$ and 100 rad/s, the χ_2 -phase (phase-line network) is shear-thinning coherently in the rubbery plateau, but the χ_1 -phase is still incoherent. For ω between 100 and 200 rad/s, both dual-phases are stretching coherently, a condition that may have consequences for the long-term stability of the deformed state obtained. This type of experiment and analysis with the dual-phase model, we suggest, must be sys-

tematically accomplished to understand the impact of thermo-mechanical treatments, such as “rheo-fluidification”, also called “disentanglement” (Chapters 2 and 4, refs [40, 41]), on the long-term stability of new states for the entanglement network.

In Figure 5.97, we study the variation of the activated strand coherence factor, k , as a function of ω for the polystyrene melt of Figure 5.25 analyzed at $T = 150^\circ\text{C}$ and 2% strain. The reason for lowering the temperature is to make apparent the maximum of the melt elasticity, $\chi = (G'/G^*)^2$, within the range of frequencies studied. For $\omega = 0.01$ to ~ 7 rad/s, the value of k is constant at 0.5. This range corresponds, in Figure 5.25, to the left of the maximum of $(G'/G^*)^2$, the value of k starting to deviate at exactly the value of ω for the maximum.

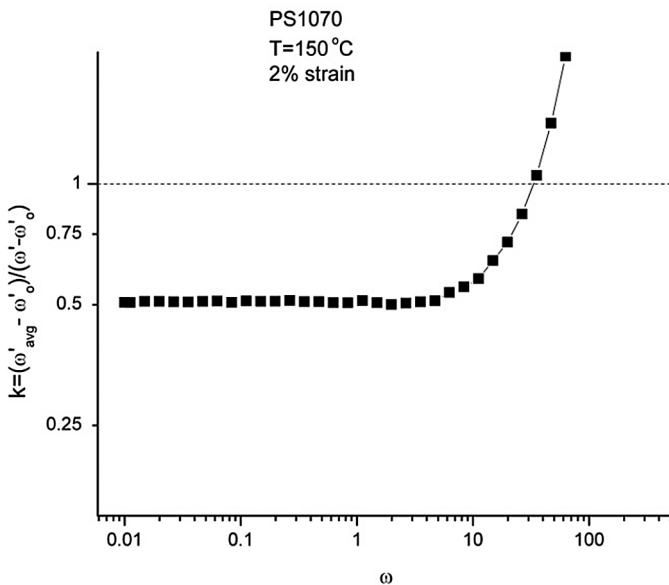


Figure 5.97 Plot of the activated strand coherence factor, k , vs ω for PS at $T = 150^\circ\text{C}$, 2% strain. Same data as in Figure 5.25

When ω is greater than 7, k quickly rises with ω and becomes 1 for $\omega \sim 37$ rad/s. The meaning of Figure 5.97 is that k only remains constant over a restricted range of frequencies, up to the maximum of the melt elastic stored energy. The points located above the horizontal line $k = 1$ cannot physically be larger than 1 so that, in fact, they remain equal to 1 once k has reached this value. Eq. (5.16) controlled the mechanism of deformation while k was constant and remained valid in the regime where k increased to 1, yet is now in default for the points above the $k = 1$ line. We assume, first, that Eq. (5.14) remains valid but now applies to a modulus, $G^{*(2)}$, that defines deformation in the χ_2 -phase; second, that there is another com-

As said in the preamble, it is a goal of the research that led to the writing of this book to set new grounds for the understanding of polymer properties using the new concepts of grain-field statistics. Interestingly, or perhaps annoyingly for the reader, the equations describing this new open dissipative interactive systems statistics are not given explicitly in the book. This was a deliberate choice, because they are the subject of a totally different book that explores the mathematical ramifications of the original assumptions and concepts. The decision was made to remain intuitive in defining the dual-phase and cross-dual-phase systems by sketches and cartoons instead of mathematical formulas and simulations. Nevertheless, the analogies through cartoon sketches explain rather simply the interactive coupling in polymers, from the solid state to the liquid state, from flow to molecular motions, for amorphous and crystalline materials. In particular, the program of research explored in the book is set to determine how the new statistics can not only explain all the classical properties of polymers (Chapter 5) but also “sustained-orientation”, which classical models cannot explain, and predict the conditions to successfully prepare “plastic battery materials”, an application described below.

■ 8.2 Industrial Applications: Improve the Processability of Existing and New Resins

The plastics industry is the source of 4% of the total worldwide energy consumption and Europe takes a share of approximately 20% of the total production of plastic materials. The industry’s main problem relates to the high viscosity of molten plastics, which in turn leads to high energy consumption during processing. Large resources are invested all over the world every year to improve the processability of existing and new resins.

This book is the result of trying to understand “disentanglement technology”, i.e., the development of engineering processing solutions that substantially decrease the viscosity of melts, allows them to be processed at lower temperatures, under low pressure, without or with much less degradation, and with improved dispersion when additives are compounded. By implementing “disentanglement technology” into standard and established industrial procedures, the temperature needed to process polymers can be reduced by 50–100 °C, which has a significant impact on the reduction of energy consumption to produce plastics and compounds. All these benefits of “disentanglement technology” were real, quantified, yet they were not understood; worse, they contradicted the established understanding.

It took me about 10 years of academic research to come up with a different model to explain the source of molecular motions and flow in polymers compatible with the sustained-orientation results. The driving force behind this research was not to create a new theory in polymers, it was the comprehension – against all the rejections by my peers – of practical results that allowed the processing of polymer melts at higher throughputs, with less degradation and with a lower energy cost, to obtain better and cheaper finished products. It did not take me long to realize that the key to make all these processing benefits happen was a better understanding of entanglements, its relationship to viscosity, and the understanding of viscoelasticity with respect to polymer interactions. These were the keys to open up a new world of entanglement manipulation technology to obtain, in particular, a significant reduction of the viscosity of the melt (by “disentanglement”).

This new understanding of polymer interactions and entanglement expresses a paradigm shift in polymer physics that leads to a roster of new innovative applications (see Appendix A: Rheo-fluidification Markets).

The “disentanglement technology of the first generation” has already had an immense impact in specific industrial areas such as in the extrusion of plastic melts at lower temperatures with a 40% throughput increase, the increase of permeability in films for the food industry, improved dispersion of nanoparticles in polymer melts, processing under a much lower pressure and at a lower temperature with an identical throughput, increase of productivity and cost reduction for injection molding, extrusion and compounding lines, extrusion for the pharmaceutical industry, biomaterial fabrication for the medical industry (electro-spinning-writing), and the 3D printing industry etc. For instance, the high temperatures necessary for processing plastics (in extrusion or injection molding) prevent the pharmaceutical industry from incorporating temperature-sensitive active pharmaceutical ingredients into pharmaceutical grade polymers, which is a very innovative approach that has attracted significant interest in pharmaceutical technology. The new understanding of flow in entangled polymers explains how to “disentangle” melts, reduce their viscosity drastically, and process them at low temperatures to make it feasible.

Pink-Flow Technology

What I call “pink-flow” technology describes the second generation of machinery, processes, and new materials produced following this new understanding of the parameters to control the “entanglement stability” of polymer melts.

The first generation of “disentangles” was very useful to discover “sustained-orientation” and to address its obvious immediate applications. However, the first generation machines had two problems: the first one was the necessity to increase the length of the disentangling hardware as the throughput increased. This made

Index

Symbols

3.4 power exponent 48
(c,g,t) statistics 373

A

accuracy consideration 40
activated phase-lines coherence factor 272
Arrhenius behavior 301
art and science of disentanglement technology 236

B

b and F types of conformers 6
b-conformers 10
b/F duality 393
b/F statistics 12, 373
b-grain glassification 397, 401
b-grains 8
blinking
– factor or constant 350
blinking mechanism 16, 18, 392, 400, 401
blinking mode 18
blinking network activation 412
bonded conformer 6
Boyer 283, 284, 292, 302, 383
Boyer's T_l,I relaxation 292

C

challenge to the reptation model 403
classical Maxwell rules 373
classical view 2
classical viscoelasticity theory 409
closed-loop (inactive) dual-phase strand 371
cohesive network energy 292
combination of shear-flow and extensional flow 101
combined flow rates
– from pressure flow and rotational flow 102
combined oscillation and rotation 108
concept of entanglement 411
conformational isomeric state 277
conformational state of the conformers 411
conformers 6
core-phase 257, 258, 276, 277, 279, 321, 328–330, 336–340, 343, 354, 363, 367, 368, 372, 376–378, 381
Cox-Merz rule 35
Cross-Carreau formula 34
cross-dual-phase
– symbolism 377
cross-dual-phase entanglement network 15, 264
cross-dual-phase model 4, 365, 376, 378–380, 382
crossed dual-Phase statistics 13

D

data sources 36
 de Gennes 34, 375, 383
 departure from superposition
 – lower melt temperature 67
 – upper melt temperature 63
 design of the ribs 24
 dielectric and dynamic mechanical measurements, simultaneous 226
 disentangled melts 25
 – in-line viscosity 230
 disentangled pellets 25
 – melt flow index 230
 disentangled polymers
 – properties 232
 disentanglement 18, 261, 274, 280, 296, 310, 327, 340, 351, 353, 378, 404, 410, 413
 disentanglement parameters 421
 disentanglement processors 230
 disentanglement treatment 261
 disentanglers 420
 dissipative factor 12
 dissipative function 12
 dissipative stability of a cross-dual-phase melt 411
 dissipative systems 425
 drooling 213
 dual-phase disentanglement 413
 dual-phase explanation
 – of solid-like elasticity 400
 Dual-Phase model 4
 dual-phase statistics 411
 dual-phase structure 259
 dual-split statistics 8
 dual-split statistics view 3
 dynamic free volume 19
 dynamic frequency of the entanglement network 258
 dynamic structure of entropy 382

E

edge fracture 113, 216

effect of strain amplitude on the structure of the entanglement network 263
 effect of the surface on the viscoelastic response 227
 elastic dissipative 385
 elastic dissipative melt 397
 elastic dissipative nature of the interactions 401
 elastic dissipative phase-wave 398
 elastic dissipative state 385
 elasticity of the network of entanglements 257
 elastic sweeping wave 412
 electrostatic interactions 7
 energy storage materials 421
 energy stored by the network of activated phase-lines 257
 entanglement instability 28
 entanglement network instability 202
 – long term 199
 entanglement phase 15, 265
 entanglements 2, 3, 32
 – new interpretation 417
 entanglement stability on crystallization 423
 entanglement state 16
 entropy of the dual-phase network 265
 equations of rheology 44
 experimental procedures 116
 Eyring modelization of flow 272

F

famous rock band of the 1970s 421
 F-conformers 10, 276–278, 291, 365–367, 401
 flow improvement 27
 fluctuating standing wave 18
 fracture of the network 275
 free conformer 6
 free volume 31, 33, 40, 48, 52, 66, 75
 frequency for sweeping wave 18
 frequency map 283

frequency sweeps 301
frequency–time–frequency (FTF) experiment 117
FT1–FT2–FT1–FT2 (four-step) experiment 117
fully oriented cross-dual-phase 372

G

GLaMM model 407
glassy-like melt 397
grain-field statistics 15, 28, 259, 265, 277, 291, 341, 366, 367, 377, 401, 411, 425
grain-classification 11

I

impact in specific industrial areas 420
industrial applications 419
in-pellet disentanglement 235, 280
in pellets
– retention of viscosity reduction 413
instability of the network of entanglement 29
intermittent process of stretch–relax 294

K

kinetics of the re-entanglement process 234

L

linear viscoelasticity 379
low ω tail 387, 389

M

macro-coils 13
melt behavior at low frequency 359
melt disentanglement treatment 235
melt elasticity 264, 274, 278, 279, 297, 298, 313, 320, 330, 335, 337, 344, 349, 353, 354, 360

melt entanglement stability 89
– research 425
melt fracture 113
melt fracture initiation 224
melt stored elasticity 274
MFI 280, 310
MFI measurement 120
molecular dynamics 409
molecular weight and temperature effects separate 33
momentum of the elastic dissipative phase-wave 397

N

natural sweeping wave frequency of the entanglement phase 258
nature of entanglement 236
network elasticity 276, 278, 286, 287, 293, 296, 298, 321, 337, 351, 365
network of entanglement 258
network strain elastic energy 16
new entanglement states 249
New School Polymer Physics 421, 422, 424
Newtonian viscosity
– accuracy in determination 54
new understanding of entanglements 413, 424
new understanding of the concept of entanglements 248
non-Newtonian viscous behavior 34
number of phase-lines unconnected to the network 264

O

onset of entanglements 259
orientation of the phase-lines 257

P

paradigm shift in polymer physics 420
phase-lines 15, 257
phase-line sweeping mechanism 350

- phase-wave 18
 - static and dynamic frequency 265
 - physics of interlocking scales 382
 - pink-flow technology 420
 - plastic-fuel-battery 421
 - plastification 215
 - plateau modulus 287
 - polymer characterization 116
 - polymer melt
 - flow properties 15
 - molecular interactions 15
 - polymer melt deformation 236
 - pseudo-plasticity 26
 - pure viscometry test 117
 - pure viscometry test followed by frequency sweep 117
- R**
- Rabinowisch's formula 38
 - reptation 285, 379
 - reptation model of de Gennes 34
 - reptation theoretical model 405
 - rheo-fluidification markets 426
 - Rheo-Fluidification processor 22
 - Rheo-Fluidizer 22
 - rheological parameters
 - definition to analyze melt stability 122
 - Rheo-SANS
 - Noirez's results 404
 - Watanabe's results 403
 - Rheo-SANS evidence by Zhe Wang et al. 405
 - ribs 22
 - rotation and oscillation shear modes
 - combining 98
 - Rouse's model 52
- S**
- shear degradation 211
 - shearing of a melt
 - in our model (summary) 296
 - shear-refinement
 - effect of thermal-mechanical history 110
 - shear-refinement into pellets 229
 - shear-refinement under dynamic conditions 100
 - shear-thickening 288
 - shear-thinning 2, 3, 34, 216, 257–259, 272, 275, 276, 278, 280, 287, 288, 291, 297, 298, 310, 311, 320–322, 324, 327, 328, 333, 340, 343, 344, 348, 350–352, 354, 356, 357, 363, 367, 368, 371, 373, 376–378, 386, 387, 389, 392, 400, 401, 403
 - solid-like behavior 385
 - solid-like melt
 - elasticity 400
 - solid-like results 388
 - spectrum of relaxation 73
 - spherical harmonic expansion 406
 - split of the statistics 411
 - stability of entanglements 423
 - stability of the network 217
 - stability of the network of entanglement 249
 - stability of the network of interactions 259
 - stability of the state of interactions 385
 - stable entanglement state 249
 - step strain experiment 90
 - step strain rate experiments 94
 - stored elasticity in the melt 390
 - strain
 - effect of 322
 - strain-induced transients under oscillatory shear 96
 - strain softening 258
 - strands of the network of channels 294
 - stretch-relax mechanism 16, 258, 265, 271, 272, 292, 341, 343, 345, 348, 351, 356, 357, 359, 360, 367, 370, 373
 - st-t conformational state 12
 - superposition principle
 - validity 71
 - surface effect 398
 - surface melt contact 227

sustained-orientation 21, 23
sustained oriented entanglement
states 250
sweeping mode 18
sweep wave frequency 257

T

temperature dependence on the polymer
type 313
temperature ramp down experi-
ments 296
terminal time 217
time sweep 127
– simple 116
– simple, then cooling ramp test 116
time-temperature superposition 59
TLL temperature 302, 310, 355
trans conformers 277, 292, 294, 367,
369, 370, 373
transient and steady state behavior 89
transients and steady states 249
tube model 407

V

van der Waals interactions 7
Vinogradov shifting 291
Vinogradov's melt fracture criteria 224
Vinogradov's plot 35
visco-elasticity 2, 3
viscoelastic parameters
– origin of time dependency 210
viscosimetric experiments 130
viscosity measurement
– in-line 118
viscosity measurement under extrusion
flow conditions 118
viscous heating 211
Vogel-Fulcher equation 48, 281, 298
Vogel-Fulcher's formulation 395

W

WLF constants 44
WLF equation 31, 281, 298, 321, 375
working at constant free volume 411